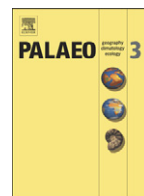




Contents lists available at SciVerse ScienceDirect

Palaeogeography, Palaeoclimatology, Palaeoecology

journal homepage: www.elsevier.com/locate/palaeo

Coeval Eocene blooms of the freshwater fern *Azolla* in and around Arctic and Nordic seas

Judith Barke^{a,b}, Johan van der Burgh^b, Johanna H.A. van Konijnenburg-van Cittert^{b,c,*}, Margaret E. Collinson^d, Martin A. Pearce^e, Jonathan Bujak^f, Claus Heilmann-Clausen^g, Eveline N. Speelman^h, Monique M.L. van Kempenⁱ, Gert-Jan Reichart^h, André F. Lotter^a, Henk Brinkhuis^b

^a Palaeoecology, Laboratory of Palaeobotany and Palynology, Department of Physical Geography, Utrecht University, Budapestlaan 4, 3584 CD Utrecht, The Netherlands

^b Marine Palynology Group, Laboratory of Palaeobotany and Palynology, Department of Earth Sciences, Utrecht University, Budapestlaan 4, 3584 CD Utrecht, The Netherlands

^c National Centre for Biodiversity-Naturalis, PO Box 9517, 2300 RA Leiden, The Netherlands

^d Department of Earth Sciences, Royal Holloway University of London, Egham, Surrey, TW20 0EX, UK

^e Statoil, 2103 City West Boulevard, Houston, TX 77042, USA

^f Bujak Research International, 288 Newton Drive, Blackpool, FY3 8PZ, UK

^g Geologisk Institut, Aarhus Universitet, DK-8000 Aarhus C, Denmark

^h Geochemistry, Department of Earth Sciences, Faculty of Geosciences, Utrecht University, Budapestlaan 4, 3584 CD Utrecht, The Netherlands

ⁱ Department of Aquatic Ecology and Environmental biology, Faculty of Science, Radboud University, Heyendaalseweg 135, 6525 AJ, Nijmegen, The Netherlands

ARTICLE INFO

Article history:

Received 12 September 2011

Received in revised form 28 March 2012

Accepted 2 April 2012

Available online xxxx

Keywords:

early middle Eocene

Arctic Ocean

Nordic seas

Azolla

Fresh ocean surface waters

EECO (Early Eocene Climatic Optimum)

ABSTRACT

For a short time interval (c. 1.2 Myr) during the early middle Eocene (~49 Myr), the central Arctic Ocean was episodically densely covered by the freshwater fern *Azolla*, implying sustained freshening of surface waters. Coeval *Azolla* fossils in neighboring Nordic seas were thought to have been sourced from the Arctic. The recognition of a different *Azolla* species in the North Sea raised doubts about this hypothesis. Here we show that no less than five *Azolla* species had coeval blooms and spread in the Arctic and NW European regions. A likely trigger for these unexpected *Azolla* blooms is high precipitation prevailing by the end of the warmest climates of the Early Eocene Climatic Optimum (EECO).

© 2012 Elsevier B.V. All rights reserved.

1. Introduction

High concentrations of megaspores and microspore massulae of the free-floating freshwater fern *Azolla arctica* were recovered from basal middle Eocene (~49 Ma) central Arctic Ocean sediments drilled at the Lomonosov Ridge during the Arctic coring expedition (ACEX; or Integrated Ocean Drilling Program, IODP, Expedition 302; Backman et al., 2006; Brinkhuis et al., 2006; Collinson et al., 2009). The co-occurrence of different life-stages and reproductive parts of *A. arctica* and the absence of land-plant detritus suggest that this floating fern grew and reproduced *in situ* on the central Arctic Ocean surface (Brinkhuis et al., 2006; Collinson et al., 2009), waxing and waning with the obliquity (~40 kyr) cycle for

some 1.2 Myr (Speelman et al., 2009; Barke et al., 2011). Extant species of *Azolla* grow exclusively on freshwater bodies, such as ponds and lakes in tropical, subtropical, and warm temperate regions. Cultivation experiments (by MMLvK) show that *Azolla filiculoides* tolerates salinities of only up to 5 psu. Associated facies of *Azolla* fossils, the oldest one dating back to the Late Cretaceous, are in complete support of their exclusive growth in freshwater settings (Collinson, 2001, 2002). This strongly implies that central Arctic Ocean surface waters were fresh enough to sustain the growth of this freshwater fern. Associated findings with the *Azolla* corroborate the episodic presence of fresh surface waters, strong stratification, and bottom water anoxia (Brinkhuis et al., 2006; Stein et al., 2006; Onodera et al., 2008; Stickley et al., 2008; Waddell and Moore, 2008; Barke et al., 2011).

Abundant *Azolla* remains have previously been reported from basal middle Eocene marine deposits in the sub-Arctic and Nordic seas, where they were mainly recognized in hydrocarbon exploration wells (Brinkhuis et al., 2006; Speelman et al., 2009). These coeval occurrences in the Nordic Sea deposits were suggested to represent transported

* Corresponding author at: Palaeoecology, Laboratory of Palaeobotany and Palynology, Department of Physical Geography, Utrecht University, Budapestlaan 4, 3584 CD Utrecht, The Netherlands. Fax: +31 302535096.

E-mail address: j.h.a.vankonijnenburg@uu.nl (J.H.A. van Konijnenburg-van Cittert).

assemblages of *Azolla arctica* from the Arctic Ocean by freshwater spills (Brinkhuis et al., 2006; Collinson et al., 2009). However, recent palaeobotanical examinations of the *Azolla* assemblage at the southernmost Nordic Sea site in Denmark revealed the presence of a second *Azolla* species, *Azolla jutlandica* (Collinson et al., 2010). This intriguingly suggests that *Azolla* blooms, involving at least two species, occurred contemporaneously over a wide area and along a large latitudinal gradient. There are various hypotheses that may explain this phenomenon: i) different species of *Azolla* grew in different areas *in situ* on ocean surfaces, ii) *Azolla* grew *in situ* in the central Arctic Ocean and was transported to other oceanic settings by freshwater spills from e.g. the central Arctic Ocean; this explanation cannot apply to the Danish occurrence as the species is different, iii) *Azolla* remains at marine settings other than the central Arctic Ocean site were transported from adjacent land.

To test these hypotheses, and their implications, we selected thirteen sites along a north-to-south transect, between the Arctic Ocean and southern North Sea, plus four sites in the western Arctic Ocean (see Fig. 1; Table 1). We investigated the time equivalence of the basal middle Eocene *Azolla*-bearing interval between locations and determined the *Azolla* species composition and abundance per site (Tables 2 and 3). In order to better understand the depositional processes and environmental conditions at the various sites the composition of the total palynomorph assemblage has been assessed and the amount of terrestrially-derived mesofossils (wood, fusain and cuticles >250 µm) has been estimated (Table 3).

2. Materials and methods

2.1. Palynology

The sediment samples were oven-dried at 60 °C. *Lycopodium clavatum* tablets containing a known number of spores were added. Samples were treated with HCl (30%) and cold HF (40%) with no oxidation and sieving with a 15 and 250 µm mesh (for details see Wood et al., 1996). Slide-mounted residues (size fraction between 15 and 250 µm) were examined under the light microscope. For percentage calculation (JB) of total *Azolla* (species undifferentiated), peridinooid dinocysts, gonyaulacoid dinocysts, non-saccate pollen, bisaccate pollen and spores a minimum of 100 palynomorphs were counted. Pollen and spore identification was based on Moore et al. (1991). Dinocysts were identified following nomenclature cited in Fensome and Williams (2004); environmental interpretations from dinocysts followed Pross and Brinkhuis (2005), Sluijs et al. (2005, 2008), and Sluijs and Brinkhuis (2009). Total *Azolla* counts were based on complete and partial massulae; due to their spongy structure with preformed divisions, it is impossible to distinguish complete from partial massulae. Isolated glochidia were not counted. Absolute quantitative numbers of *Azolla* massulae were calculated using the relative number of *Lycopodium* spores.

For percentage calculation of individual named *Azolla* species (Table 3 right columns) all the massulae or massula fragments (only



Fig. 1. Study sites (modified from www.google-earth.com). JMFZ = Jan Mayen Fracture Zone; GIR = Greenland Iceland Ridge; IFR = Iceland Faroe Ridge; Faroe Isl. = Faroe Islands.

Table 1

Site descriptions. The *Azolla* material from site 5 (IODP 302-4A) has been fully documented in Collinson et al. (2009). The *Azolla* material from site 16 (Kirstinebjerg) has been fully documented in Collinson et al. (2010). BMB = Beaufort Mackenzie Basin; mMD = meters measured depth; mbsf = meters below sea floor. The material studied comes from multiple sample levels within the *Azolla* interval at sites 5, 6 and 7, where coring material was available. At sites 1–4 and sites 8–15 the studied material derives from wells. At sites 16 and 17 it derives from outcrops.

Area	Location	Site	Name (operator)	Position	<i>Azolla</i> -bearing horizon	Sampling depth	Sample weight (g)	# megaspores studied
Western Arctic	Northern Alaska	1	Sandpiper 1 (Shell)	70°35'4.73"N/149°5'48.82"W	1070–1097 mMD	1088–1097 mMD	16	19
		2	Northstar 1 (Amerada)	70°31'42.02"N/ 148°51'22.51"W	1088–1143 mMD	1088–1116 mMD	10	13
	Canadian BMB	3	Ellice I-48 (Chevron et al.)	69°7'34.00"N/ 135°55'33.50"W	1910–2075 mMD	1910–1915 mMD & 1940–1945 mMD	23	19
		4	Upluk M-38 (Chevron sobc)	69°27'56.00"N/ 135°24'54.00"W	3182–3292 mMD	3237–3240 mMD	22	3
Central Arctic Nordic seas	Lomonosov Ridge	5	IODP 302-4A	87°51'59.69"N/ 136°10'38.46"E	298.8–302.6 mbsf	298.9–302.6 mbsf (with 10 cm spacing)	1 to 2	details in Collinson et al., 2009
	Norwegian-Greenland Sea	6a	ODP 151-913B	75°29'21.12"N/ 6°56'48.48"W	674.8–717.6 mbsf	684.4 mbsf	13	6
		6b				687.9 mbsf	13	4
		6c				694.2 mbsf	13	0
		6d				694.7 mbsf	14	6
		7a	ODP 104-643A	67°42'54.00"N/1° 1' 59.88"E	556.0–565.3 mbsf	563.7 mbsf	12	9
		7b				564.7 mbsf	13	10
		7c				564.8 mbsf	12	3
		8	6610/2-1 S (Statoil)	66°48'48.73"N/ 10°30'26.70"E	As for sampling depth	1240 mMD	13	11
	North Sea	9	6608/10-10 (Statoil)	66°4'17.90"N/ 8°10'11.40"E	As for sampling depth	1760 mMD	12	0
		10	6507/8-4 (Statoil)	65°23'17.18"N/ 7°23'59.65"E	As for sampling depth	1920 mMD	8	6
		11	6506/11-6 (Statoil)	65°1'26.24"N/ 6°25'10.71"E	As for sampling depth	2240 mMD	13	0
		12	6406/2-2 (Statoil)	64°49'46.35"/ 6°34'15.43"E	As for sampling depth	2370 mMD	15	18
		13	6302/6-1 (Statoil)	63°31'38.43"N/ 2°45'51.56"E	As for sampling depth	3180 mMD	12	12
		14	30/2-1 (Statoil)	60°52'05.42"N/ 2°38'49.16"E	As for sampling depth	1860 mMD	14	0
		15	16/4-4 (Statoil)	58°31'47.81"N/ 2°8'59.69"E	As for sampling depth	2020 mMD	14	6
		16	Kirstinebjerg	5°35'49.97"N/ 9°48'06.48"E	~2.8 m thick horizon in outcrop	Sample 2904	29	Details in Collinson et al., 2010
17		Kasmose	55°33'16.89"N/ 9°50'05.65"E	~2.8 m thick horizon in outcrop	Sample 2903	25	0	

Table 2

Distinctive microspore massula characteristics of *Azolla arctica*, *Azolla jutlandica*, *Azolla* sp. 1 and *Azolla* sp. 2. There is no record of microspore massulae for *Azolla* sp. 3 (see explanation to Table 3). Measured distances for features lettered (A)–(E) are shown in Fig. 3.

Distinctive microspore massula characteristics which differ between <i>Azolla arctica</i> , <i>Azolla jutlandica</i> , <i>Azolla</i> sp. 1 and <i>Azolla</i> sp. 2				
	<i>Azolla arctica</i>	<i>Azolla jutlandica</i>	<i>Azolla</i> sp. 1	<i>Azolla</i> sp. 2
Width of glochidia anchor-tips (A)	4–5 µm	up to 8 µm	8–9 µm	6–7 µm
Width of glochidia shafts (B)	2–2.5 µm	5–8 µm	3–4 µm	3 µm
Width of lower part of glochidia stalks (C)	1 µm	2 µm	2 µm	2 µm
Length of glochidia flukes (D)	2–3 µm	6 µm	5 µm	up to 5 µm
Length of glochidia fluke extensions (E)	0.5–1.5 µm	1.5–2.5 µm	4–6 µm	2–4 µm
Total length of glochidia (F)	22–30 µm 45–85 µm	15–55 µm	45–85 µm	30–75 µm
Shape of glochidia anchor-tips	Rounded	Typically broad, flat and blunt-ended	Obtusely rounded	Broad and flat to rounded to arrow head-shaped
Shape of glochidia fluke tips	Not recurved	Not recurved	Typically recurved	Straight; sometimes recurved
Attachment of glochidia stalks to massulae	Stalk width unchanged at attachment area	Stalk width widening slightly	Stalk expanding to wide attachment	Stalk width widening slightly
Hairs on lower glochidia stalks (length)	Absent	Sometimes (2–5 µm)	Often (3–4) µm	Absent
Hairs on massulae (length)	1–2(3) µm	2–5 µm	3–4 µm	absent
Length of laesurae	2/3 radius	1/3 radius	1/2 radius	1/2 radius

those with glochidia tips attached) contained within two palynological slides were counted per sample (JvdB). Isolated glochidia were not counted. Some samples contained only a few massulae; in these cases the actual number of massulae counted is indicated in brackets below the percentages (see Table 3).

2.2. Palaeobotany

The >250 µm size fraction of the sample residues was studied under the dissecting microscope. Mesofossils encountered in these residues include wood, fusain, cuticles (together grouped as terrestrially-derived mesofossils) and *Azolla* remains (megaspore apparatuses and clusters of microspore massulae). The abundance of terrestrially-derived mesofossils is categorized as present (–), rare (+), frequent (++) and common (+++); see Table 3. A selection of megaspore apparatuses, representative of the range of morphologies seen in the sample, was picked and studied by scanning electron microscopy (SEM). The number of megaspore apparatuses studied per site is indicated in Table 1. Some of the megaspore apparatuses had attached microspore massulae which were also studied by SEM as were some isolated massulae clusters. Specimens studied by SEM were processed following the method described in Collinson et al. (2009, 2010).

The slide-mounted residues and mesofossil material studied are housed in the Laboratory of Palaeobotany and Palynology (Utrecht).

2.3. Age assessment

The maximum duration and absolute ages of the *Azolla*-bearing horizon are inferred from the Ocean Drilling Program ODP Leg 151 Site 913 and are based on the Gradstein et al. (2004) timescale (Speelman et al., 2009). The last abundant occurrence (LAO) of *Azolla* in the composite section developed from Holes DSDP Leg 38 Site 338, ODP Leg 104 Site 643A and ODP Leg 151 Site 913B has been shown to coincide with the last consistent occurrence (LCO) of *Eatonicysta ursulae* and is directly calibrated against mid Chron C21r (Eldrett et al., 2004). Based on this calibration and using the timescale by Gradstein et al. (2004), the top of the *Azolla* bearing horizon is dated at 48.1 Ma (Speelman et al., 2009). In Core 913B *Azolla* is still present near or at the base of Chron 22n. The low abundances of *Azolla* at the base of the core suggest the closeness to the onset and have been shown to correspond to the LAO of *Eatonicysta ursulae* within Chron C22n (Brinkhuis et al., 2006). Using the timescale by Gradstein et al. (2004), the onset is dated at approximately 49.3 Ma, giving a total duration of 1.2 Ma for the entire *Azolla* interval (Speelman et al., 2009).

3. Biostratigraphy and correlation

3.1. Western Arctic Basin sites: Northern Alaska and Canadian Beaufort Mackenzie Basin (sites 1–4, see Table 1)

The basal middle Eocene *Azolla* horizon has been recognized in more than 100 commercial wells in Northern Alaska and the Canadian Beaufort Mackenzie Basin (BMB), and is documented in an informal palynological zonal scheme (Bujak Research International, unpublished data). This zonal scheme is based on the last occurrences of dinocysts, fungi, pollen and spores and comprises zones from the Paleocene (T1) to the Oligocene (T6). In all wells, the basal middle Eocene *Azolla* horizon occurs in the same biostratigraphical position, namely in the palynological subzone T4a, which is characterized by the abundant occurrence of the dinocyst *Charlesdownia tenuivirgula*. This subzone belongs to zone T4 (middle Eocene), which is characterized by the abundant occurrence of the fungus *Pesavis tagaluensis*. The index dinocyst species that have stratigraphical importance for the basal middle Eocene succession in the Nordic Seas (Bujak and Mudge, 1994; Eldrett et al., 2004), are all absent probably due to an intolerance to brackish conditions in the Arctic (Brinkhuis et al., 2006).

Furthermore, the Northern Alaskan wells include the uppermost Paleocene *Apectodinium* horizon, which corresponds to the upper part of zone T2 (latest Paleocene) and relates to the global PETM. Both the PETM and the *Azolla* horizon are characterized by a distinctive high-gamma curve in the Northern Alaskan wells. These markers are absent from the Canadian Beaufort Mackenzie Basin wells, probably due to the strong depositional influence of the Mackenzie delta. The uppermost Paleocene *Apectodinium* horizon and the basal middle Eocene *Azolla* horizon are the only chronostratigraphical correlations available that allow us to correlate from the Arctic to the Nordic latitudes.

3.2. Central Arctic Ocean site: the Lomonosov Ridge (site 5, see Table 1)

The *Azolla* bearing horizon in core M0004-11X, drilled during the Arctic Coring Expedition (ACEX) or Integrated Ocean Drilling Program (IODP) Expedition 302, is bracketed by the same dinocyst events as the basal middle Eocene *Azolla* horizon in the Canadian BMB wells. The late Paleocene/early Eocene to middle Eocene dinocyst succession, informally described for the Canadian BMB wells, includes the following events: *Apectodinium* acme and *Glaphrocysta ordinata* prior to the *Azolla* acme event and *Operculodinium cf. tiara* and *Cribroperidinium tenuitabulatum* following this event (Bujak Research International, unpublished data). As in the Canadian BMB wells, the age-diagnostic dinocyst markers of the Nordic Sea succession are absent from the ACEX cores and furthermore no palaeomagnetic data are available (Backman et al., 2006). However, correlation of the last abundant occurrence (LAO) of *Azolla* in the Arctic with the last abundant occurrence (LAO) of *Azolla* in ODP Hole 913B (Brinkhuis et al., 2006) is consistent with the current age model of the Paleogene ACEX cores (Backman et al., 2006; Brinkhuis et al., 2006).

3.3. Nordic Sea sites: Norwegian–Greenland Sea and North Sea (sites 6–17, see Table 1)

The main bioevents of the Eocene succession in the Norwegian–Greenland Sea have been calibrated against magnetostratigraphy. This magnetobiostratigraphic calibration is based on the composite section developed from Holes DSDP Leg 38 Site 338, ODP Leg 104 Site 643A and ODP Leg 151 Site 913B. Hence, site 6 (ODP 104-643A) and site 7 (ODP 151-913B) contain the *Azolla* bearing horizon, the age diagnostic dinocyst markers as well as paleomagnetic data. The last abundant occurrence (LAO) of *Azolla* in this composite section has been shown to coincide with the last consistent occurrence (LCO) of *Eatonicysta ursulae* and is directly calibrated against mid Chron C21r (Eldrett et al., 2004). The interval of abundant *Azolla* correlates with the last occurrence (LO) of *Charlesdownia columna* (Brinkhuis et al., 2006), which is directly correlated to the top of Chron C22n (49 Ma; Eldrett et al., 2004). Although the onset of the *Azolla* horizon has not been recovered, the low abundances of *Azolla* at the base of the core suggest that this level is close to the onset. This level corresponds to the LAO of *Eatonicysta ursulae* within Chron C22n (Brinkhuis et al., 2006).

The *Azolla*-bearing horizon at sites 8–15 has been recognized in commercial wells. Since these wells were studied by means of cutting samples, the *Azolla* interval can only be defined by the last occurrence (LO), last consistent occurrence (LCO) or the last abundant occurrence (LAO) of *Azolla*. In all these wells the last (abundant/consistent) occurrence of *Azolla*, is located within or at the top of the Ypresian and coincides with the LCO of *Eatonicysta ursulae* and LO of *Charlesdownia columna*. Site 12 (6406/2-2) is an exception where the LCO of *E. ursulae* is positioned slightly below the LO/LCO of *Azolla*. Moreover at sites 10 (6507/8-4) and 14 (30/2-1) *C. columna* is not present at all. Further dinocyst events relevant for the age assessment of the *Azolla* interval are the LO of *E. ursulae* and *Dracodinium pachydermum* situated above the top of the Ypresian within the Lutetian (the latter dinocyst is only present in some of the

Table 3

Shows the relative abundance (based on 100 palynomorph specimen count) of *Azolla* spp (species undifferentiated), peridinoid dinocysts, gonyaulacoid dinocysts, non-saccate pollen, bisaccate pollen and spores relative to the total palynomorphs. ^a = high proportion of *Senegalinium* spp.; ^b = high proportion of *Cerodinium depressum*, *Deflandrea* spp. *Wetzeliella* spp. and *Senegalinium* spp.; ^c = high proportion of *Phthanoperidinium* spp. and *Wetzeliella* spp. The amount of terrestrial derived mesofossils is categorized as present (–), rare (+), frequent (++) and common (+++). Relative abundances (% *Azolla* massulae) of the individual *Azolla* species (*A. arctica*, *A. jutlandica*, *A. sp. 1*, *A. sp. 2* and *A. sp. 3*) and occurrences of their megaspore apparatuses are also given based on further study of two palynology slides per sample and on the mesofossil size fraction. Some samples contained few massulae and the actual number counted is indicated in brackets below the percentages. At site 6 (ODP Leg 151 Site 913B) microspore massulae of *Azolla* sp. 2 were found below depth 694.7 mbsf. For *Azolla* sp. 3 no microspore massulae were found, probably a consequence of the overall low abundance of this species, as indicated by the very small number of megaspore apparatuses recorded. Megaspore apparatuses with attached microspore massula(e) are indicated with*; megaspore apparatuses that themselves were indeterminate, but had massula(e) attached that could be identified, are indicated with†. No microspore massulae have been found attached to the megaspore apparatuses of *Azolla* sp. 3, probably because there is no filum over the megaspore, hence no hairs in which glochidia can become entwined. All megaspores from sites 3 and 4 were covered by a surface deposit, which obscured their morphological details and made identification in most cases impossible. ^d = all sites yielded megaspores but in five cases these were not studied in detail.

Study sites	% <i>Azolla</i> spp.	% Peridinoid dinocysts	% Gonyaulacoid dinocysts	% Non-saccate pollen	% Bisaccate pollen	% Spores	Terrestrially-derived mesofossils	% <i>Azolla</i> massulae (total counts)				Megaspore apparatuses ^d				
								<i>A. arctica</i>	<i>A. jutlandica</i>	<i>Azolla</i> sp. 1	<i>Azolla</i> sp. 2	<i>A. arctica</i>	<i>A. jutlandica</i>	<i>Azolla</i> sp. 1	<i>Azolla</i> sp. 2	<i>Azolla</i> sp. 3
1 Sandpiper 1	12	26 ^a	5	43	14	0	++	15			85	√		√ [†]		
2 Northstar 1	27	12 ^a	0	48	12	1	+++	100				√ [†]				√
3 Ellice I-48	16	38 ^a	6	24	16	0	+++	4			96	√				
								(1)			(17)					
4 Upluk M-38	16	54 ^a	2	16	12	0	+++	7			93	d				
								(1)			(14)					
5 IODP 302-4A	10 to 90	5 to 50 ^a	0 to 15	5 to 30	0 to 10	0 to 10	–	100				√*				
6a ODP 151-913B 684.4 mbsf	52	13 ^b	6	3	25	1	+	92	8			√			√*	
6b ODP 151-913B 687.9 mbsf	71	25 ^b	0	0	3	1	–	100				√*				
6c ODP 151-913B 694.2 mbsf	11	73 ^a	5	0	11	0	–	34	66			d				
6d ODP 151-913B 694.7 mbsf	28	24 ^b	4	14	28	2	–	97	3			√			√*	
7a ODP 104-643A 563.7 mbsf	16	28 ^c	50	3	3	0	+	62			38	√*				
7b ODP 104-643A 564.7 mbsf	20	5 ^c	70	1	4	0	–	1			99			√		
7c ODP 104-643A 564.8 mbsf	13	14	63	4	6	0	+				100			√		
8 ST.6610/2-1 S	3	7	83	2	5	0	+	83			17			√		
								(5)			(1)					
								92			8	d				
9 ST.6608/10-10	3	3	70	10	8	6	+									
10 ST.6507/8-4	52	4	42	1	1	0	–				100			√*		
11 ST.6506/11-6	13	6	68	2	6	5	+	36	64					√ [†]		
12 ST.6406/2-2	7	9	66	10	8	0	+	44	56					√		
13 ST.6302/6-1	19	8	53	1	19	0	++	10	90					√		
14 ST.30/2-1	6	11	74	5	4	0	+				100	d				
								(3)								
15 ST.16/4-4	30	11	48	2	9	0	++				100			√		
16 Kirstinebjerg	1	7	91	0	1	0					100			√*		
17 Kasmose	3	2	93	2	0	0					100	d				

wells). Furthermore, the LO of *Deflandrea oebisfeldensis* is situated well below the LO/LCO/LAO of *Azolla* and the LO of *Apectodinium augustum* is associated with the Top of the Thanetian (Late Paleocene). In addition, there is a lithological boundary in this interval, which is positioned between the Hordaland group (Lutetian age) and Rogaland group (Ypresian age). The Rogaland group has the Tare Formation or Balder Formation at the top. These formations are dominated by volcanic tuff and called Balder to the south and Tare to the north.

Sites 16 and 17 (Kirstinebjerg and Kasmose, respectively) are in outcrops. The *Azolla*-bearing horizon spans a ~2.8 m interval at both sites. At site 16, the *Azolla* bearing horizon spans the boundary between the *Areosphaeridium diktyoplokum* Zone and the *Dracodinium pachydermum* Zone (Heilmann-Clausen, 1988) and is positioned in the middle of Bed L2 of the Lillebælt Clay Formation (Heilmann-Clausen et al., 1985). The last occurrence of *C. columna* is positioned at the zonal boundary, which is defined by the first occurrence of *D. pachydermum* (Heilmann-Clausen, 1993). The LO of *E. ursulae* is situated within the *D. pachydermum* Zone (in the lower part of Bed L4).

3.4. Age comparison of *Azolla* intervals between sites

At the Norwegian–Greenland Sea sites (sites 6 and 7) the LAO of *Azolla* coincides with the LCO of *E. ursulae* (Eldrett et al., 2004). This is consistent with the evidence from sites 8–15 where the LO/LCO/LAO of *Azolla* is associated with the LCO of *E. ursulae*. The LO of *E. ursulae* as well as the LO of *D. pachydermum* at sites 8–15 is well above the LO/LCO/LAO of *Azolla*, which is in agreement with the evidence from Kristinebjerg (site 16), where the LO of *E. ursulae* and *D. pachydermum* is well above the LO of *Azolla* (Heilmann-Clausen, 1988, 1993). At sites 6, 7, 16 and 17 the *Azolla* interval has been shown to span the LO of *C. columna*. For sites 8–15, where a continuous record is missing, the LO of *C. columna* coincides with the LO/LCO/LAO of *Azolla* and LCO of *E. ursulae*.

Despite the absence of the age diagnostic dinocyst marker species of the Nordic Sea succession in the Arctic Ocean sediments (sites 1–5), an early middle Eocene age assessment is in line with the informal palynological zonal scheme established for the western Arctic Basin (sites 1–4) (Bujak Research International, unpublished data) and with the current age model of the ACEX core (site 5) (Backman et al., 2008).

In summary, the *Azolla* bearing horizon has been shown to be contemporaneous at the different sites in the Norwegian–Greenland Sea and North Sea based on the presence of significant age-diagnostic dinocysts markers. In the Eocene Arctic Ocean, these marine

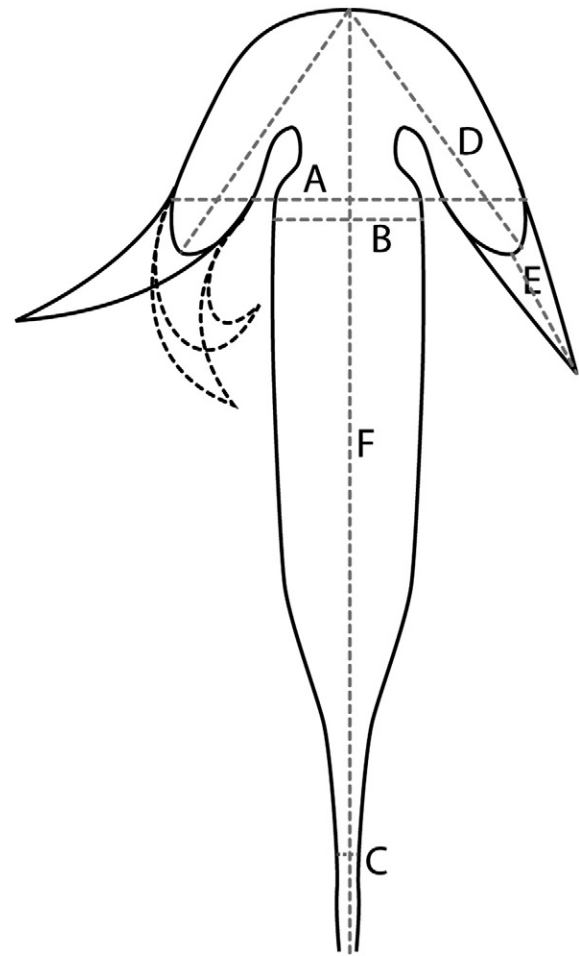


Fig. 3. Illustration of glochidium morphology and terminology. A = maximum width across glochidium anchor tips; B = width of glochidium shaft; C = width of lower part of glochidium stalk; D = length of glochidium fluke; E = length of glochidium fluke tip; F = total length of glochidium.

dinoflagellates are not recorded, probably due to an intolerance to brackish conditions (Brinkhuis et al., 2006), which hampers a direct correlation between the Nordic seas and the Arctic Ocean. However,

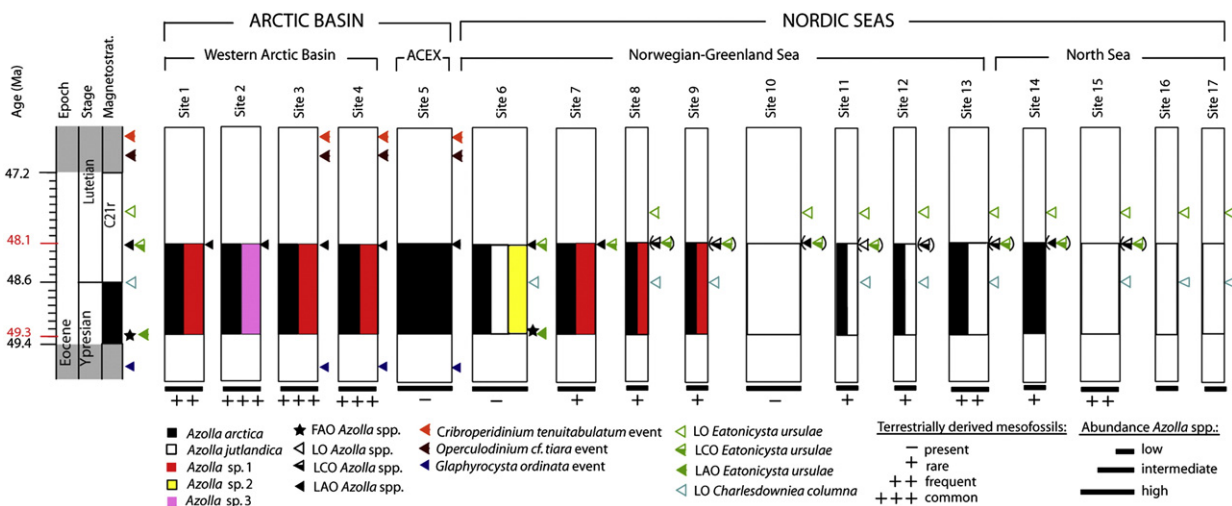


Fig. 2. Correlation panel illustrating the position of the *Azolla* interval relative to available chrono- and biostratigraphy at the various study sites. Calibration against the timescale of Gradstein et al. (2004) is obtained from site 6, ODP Site 913B. FAO = first abundant occurrence; LO = last occurrence; LCO = last consistent occurrence; LAO = last abundant occurrence. Events shown in brackets imply extrapolation from cuttings samples (see Section 3 'Biostratigraphy and correlation' for further explanation). The abundance of *Azolla* spp. is shown relative to the total palynomorph assemblage and the presence/absence of the various species of *Azolla* is indicated. Note, that raw data are provided in Table 3.

available evidence suggests that the *Azolla* blooms are at least of overlapping age (Fig. 2).

4. Paleobotanical and palynological results

4.1. Palaeobotanical results – the *Azolla* species composition

Distinctive microspore massula characteristics such as the structure of the massula, the presence/absence of hairs on its surface, the length of the laesurae of the microspores embedded within them and the measures and shapes of the glochidia that are attached to them were determined to distinguish the *Azolla* species composition at the various study sites. Surprisingly, our examinations of the various *Azolla* assemblages reveal that no less than five different *Azolla* species were present in the Arctic Ocean and Nordic Seas during the Eocene 'Azolla phase'. In addition to the previously documented *Azolla arctica* (Collinson et al., 2009) and *A. jutlandica* (Collinson et al., 2010), three additional *Azolla* species have been identified that are here referred to as *Azolla* sp. 1, *Azolla* sp. 2 and *Azolla* sp. 3. The key morphological features that distinguish the various species are summarized in Fig. 3 and Table 2 and are illustrated in Plates 1 and 2. *A. arctica* and the newly discovered *Azolla* sp. 1 occur both in the Arctic Ocean and the Nordic seas. However, at the Lomonosov Ridge in the central Arctic Ocean (site 5), only *A. arctica* is present. *Azolla* sp. 2 and *A. jutlandica* only occur in the Nordic Sea basin and *Azolla* sp. 3 is restricted to site 2 in the western Arctic Ocean. The geographical distribution of the five species is illustrated in Fig. 4 and their relative abundances are given in Table 3.

4.2. Palynological results – the palynomorph assemblage composition

In the western Arctic Basin (sites 1–4), the contribution of *Azolla* spp. to the total palynomorph assemblage ranges between 12 and 27%. Furthermore, these assemblages are rich in peridinioid dinocysts (up to 54% of total palynomorphs), dominated by the low-salinity tolerant *Senegalinium* spp. (see Sangiorgi et al., 2008; Sluijs and Brinkhuis, 2009 for review), and pollen (many non-saccate forms). In addition, gonyaulacoid dinocysts, including typical open marine taxa such as *Achomosphaera* spp., *Hystrichokolpoma* spp., *Impagidinium* spp. and *Spiniferites* spp. (see Pross and Brinkhuis, 2005; Sluijs et al., 2008 for review), occur in relatively low abundances (0–6% of total palynomorphs). The amount of terrestrially-derived mesofossils is frequent to common (Table 3). At the Lomonosov Ridge in the central Arctic Basin (site 5) the monospecific assemblage of *Azolla arctica* contributes up to 90% to the total palynomorph assemblage. Furthermore, the palynomorph assemblage comprises a high abundance of peridinioid dinocysts (up to 50% of total palynomorphs; notably the low-salinity tolerant *Senegalinium* spp.) and intermediate amounts of pollen (many non-saccate forms). Terrestrially-derived mesofossils are present (Table 3). Also at site 6 in the Norwegian–Greenland Sea, *Azolla* spp. is very abundant, contributing up to 70% to the total palynomorph assemblage. Moreover, the assemblage comprises high abundances of peridinioid dinocysts (up to 73% of total palynomorphs) containing a high proportion of low-salinity tolerant forms such as *Cerodinium depressum*, *Deflandrea* spp. *Wetzeliella* spp. and *Senegalinium* spp. (see Sluijs and Brinkhuis, 2009 for review), and intermediate amounts of pollen (both non-saccate and saccate forms). Gonyaulacoid dinocysts, including typical open marine taxa, occur in relatively low abundances (0–6% of total palynomorphs). Terrestrially-derived mesofossils are present to rare (Table 3). Also at Site 7 in the Norwegian–Greenland Sea terrestrially-derived mesofossils are present to rare and pollen occur in very low abundances (mainly saccate forms; Table 3). The *Azolla* assemblage contributes up to 20% to the total palynomorph assemblage. Moreover, the assemblage contains a high abundance of gonyaulacoid dinocysts (up to 70% of total palynomorphs) including typical open marine taxa

such as *Achomosphaera* spp., *Hystrichokolpoma* spp., *Impagidinium* spp. and *Spiniferites* spp. Peridinioid dinocysts (up to 28% of total palynomorphs) contain a high proportion of the low-salinity forms such as *Phthanoperidinium* spp. and *Wetzeliella* spp. (see Sluijs and Brinkhuis, 2009 for review). Sediments from sites 8–17 in the Norwegian–Greenland Sea and North Sea generally comprise many gonyaulacoid dinocysts and only few peridinioid dinocysts. Terrestrially-derived mesofossils are present to frequent (Table 3). *Azolla* spp. contributes between 1 and 30% to the total palynomorph assemblage and up to 50% at site 10 (for details on the palynomorph assemblage composition see Table 3).

Absolute abundances of *Azolla* are only derived for sites 5, 6 and 7, since all other sites concern commercial wells. The monospecific assemblage of *Azolla arctica* at site 5 in the Arctic Ocean contains by far the highest concentrations of *Azolla* reaching up to 324,332 massulae per gram. At sites 6 and 7 in the Norwegian–Greenland Sea total *Azolla* (*Azolla* spp.) is less abundant with concentrations of up to 95,041 (site 6) and 5865 (site 7) massulae per gram of sediment.

5. Discussion

Our palynological results (Table 3) indicate that *in situ* *Azolla* blooming is likely to explain the occurrences of *Azolla* spp. at site 5 in the central Arctic Ocean as well as at sites 6 and 7 in the northern Norwegian–Greenland Sea. At these three sites there is every indication for low-salinity surface waters (high abundance of cysts from freshwater-tolerant dinoflagellates such as *Senegalinium* spp. and *Phthanoperidinium* spp.; see Sangiorgi et al., 2008; Sluijs and Brinkhuis, 2009 for review), high abundance of *Azolla*, and rare occurrence of terrestrially-derived mesofossils. The fact that two species of *Azolla* occur at both sites 6 and 7, corroborates the presence of fresh surface waters, as it excludes the possibility that the *Azolla* occurrences represent an exceptional adaptation of a single species to normal marine salinity conditions.

Despite the strong indications for the presence of freshwater at the western Arctic sites (sites 1–4), the common occurrence of terrestrially-derived mesofossils and the relatively low proportion of *Azolla* spp. remains raise the possibility that these were washed in from nearby landmasses. At sites 8–17 in the Norwegian–Greenland Sea and North Sea the conditions were presumably not favorable for the *in situ* growth of *Azolla*, since there are no indications for a fresh surface water layer. *Azolla* spp. abundances are low to intermediate at these sites, with higher amounts of terrestrially-derived mesofossils at sites with relatively higher *Azolla* spp. abundances. This distribution pattern is likely a result of runoff and transportation from the nearby continents. Site 10, in the southern Norwegian–Greenland Sea, is an exception having high abundances of *Azolla* remains, but hardly any terrestrially-derived mesofossils. This suggests that *Azolla* remains were transported to this site from other Nordic Sea areas, e.g. from the northern Norwegian–Greenland Sea, where they likely grew *in situ*.

Absolute abundances of total *Azolla* (*Azolla* spp.) decrease with increasing distance from the Arctic Ocean (site 5 compared with sites 6 and 7; see Section 4.2). *Azolla arctica* makes up 100% of the assemblage at site 5 (324,332 massulae per gram) at site 6b (28,183 massulae per gram) and at the southern site 14 (only 3 massulae in the entirety of two slides, Table 3). These data suggest that *A. arctica* in the Nordic seas may have originated from the Arctic Ocean. Hence, a combination of all three hypotheses is likely to explain the presence of *Azolla* in early middle Eocene marine deposits; not only has this resulted from *in situ* growth of *Azolla* at various sites in the Arctic and Nordic seas as stated in hypothesis (i), but *Azolla* plants have also likely been transported by freshwater spills from e.g., the Arctic Ocean to subsequently leave their remains in the Nordic seas (hypothesis ii) or *Azolla* remains have been transported from adjacent land masses (hypothesis iii).

6. Wider palaeoecological, palaeoclimatological and palaeogeographical implications

From our results we can conclude that extensive *Azolla* blooms occurred during the same basal middle Eocene time interval on a very wide (~30 million km²) geographical scale. This implies the existence of wide-ranging continental wetlands on bordering landmasses, at least in western Canada, Alaska, and Europe, and fresh surface waters in the Arctic Ocean and in the northern Norwegian–Greenland Sea.

During the generally warm early Eocene, the hydrological cycle was intensified (Huber et al., 2003; Zachos et al., 2008; Speelman et al., 2010) and a high precipitation regime prevailed at high and mid latitudes (Pagani et al., 2006), with mean annual precipitation values of > 1200 mm/yr as e.g. estimated for Axel Heiberg Island and Greenland (Andreasson et al., 1996; Greenwood et al., 2010). Net runoff and precipitation entering the Arctic Ocean possibly amounted to 1.5×10^{13} m³/yr, which is equivalent of ~1700 mm/yr (Speelman et al., in press). The onset of the *Azolla* interval was timed shortly after the Early Eocene Climatic Optimum (EECO; 51–53 Ma), when pCO₂ was high (>2000 ppm) and global temperatures reached a long-term maximum (~12 °C global deep-sea temperature; Pearson and Palmer, 2000; Zachos et al., 2001). Climate simulations suggest that for every degree C temperature rise, global mean precipitation increases by about 2 to 3% (Held and Soden, 2006). This implies that superimposed on the overall wet conditions prevailing during the early Eocene, a further increase in precipitation is likely to have occurred during the EECO.

The Arctic Ocean was at this time nearly entirely landlocked and the connection to global oceans was restricted to a shallow surface water exchange via the Norwegian–Greenland seas (Radionova and Khokhlova, 2000; Jakobsson et al., 2007; Akhmetiev and Beniamovskii, 2009; Roberts et al., 2009). Also the Norwegian–Greenland Sea consisted of a number of isolated sub-basins, separated by the mid-ocean ridge and the Jan Mayen and Greenland–Senja fracture zones. Furthermore, it was separated from the Arctic and North Atlantic by the two major Cenozoic water mass barriers: the Yermak Plateau–Morris Jesup Rise and the Greenland–Scotland Ridge, respectively. As a result, intermediate and deep water ventilation was restricted and regional surface water exchange was poor (Eldholm et al., 1994). A sea-level low stand of approximately 20 m at ~49 Ma during Chron 21r, reported by Miller et al. (2005, Fig. 3) may have further isolated the Arctic Ocean and Norwegian–Greenland Sea basins.

The sustained and unprecedented discharge of freshwater combined with the geographical setting of the semi-closed Arctic and Norwegian–Greenland Sea basins may have created widespread fresh surface waters. Closing the seaway connections to the Arctic Basin has been simulated to result in mean Arctic surface salinities as low as ~6 psu (Roberts et al., 2009). This is corroborated by integrated climate simulations and compound-specific δD results, which suggest significant freshening of Arctic Ocean surface waters (0–6 psu) during the '*Azolla* phase' (Speelman et al., in press). These values overlap with the estimated maximum salinity tolerance of modern *Azolla* of 5 psu (by MMLvK).

The final demise of the *Azolla* is probably related to a crucial decline in high-latitude precipitation. Decreasing global temperatures in the middle Eocene (Zachos et al., 2008) likely resulted in an overall

decrease in transport of latent heat and moisture to higher latitudes (Speelman et al., 2010), diminishing the extent of continental wetlands and reducing the amount of freshwater discharge into the Arctic and Nordic seas. Even a slight increase in surface-water salinities could cross the critical threshold of salinity tolerance of *Azolla*. In addition, a possible increase in the exchange of water masses between the North Atlantic, the Greenland–Norwegian Sea basins, and the Arctic Ocean, caused by subsidence of the ridges (e.g. the eastern part of the Greenland–Scotland Ridge sank beneath sea level in the early to mid-Eocene; Thiede et al., 1996) and/or sea-level rise, may have resulted in a higher salinity of Arctic and Norwegian–Greenland Sea surface Ocean waters.

A cyclostratigraphical study on early Eocene tropical western Atlantic sediments (Demerara Rise, ODP Leg 207, site 1258) documented an ~800 kyr period of strong obliquity cycles during the middle part of magnetochron C22r (~50.1 to 49.4 Ma) and throughout the entire magnetochron C21r (Westerhold and Röhl, 2009). This obliquity pattern was interpreted to reflect a high-latitude signal, transferred to low latitudes via stronger wind-driven ocean circulation and intensification of high-latitude bottom-water formation. For the entire magnetochron C22n, which correlates to the main phase of the *Azolla* interval, no obliquity signal is detected (Westerhold and Röhl, 2009). This might be an indication that the connection from the Arctic Ocean and Norwegian–Greenland Sea to the Atlantic Ocean was indeed restricted at the time of the *Azolla* interval.

7. Conclusions

High precipitation conditions invoked by climate simulations for the Early Eocene Climatic Optimum (EECO) might have aided in the onset of massive *Azolla* proliferation in the Northern Hemisphere. No less than five *Azolla* species had coeval blooms and spread in the Arctic and NW European regions. These blooms imply the existence of wide-ranging continental wetlands on the bordering landmasses of western Canada, Alaska, and Europe, and fresh surface waters in the Arctic Ocean and in the northern Norwegian–Greenland Sea. Widespread fresh ocean surface waters were likely a consequence of the sustained and unprecedented discharge of freshwater combined with the geographical setting of the semi-closed Arctic and Norwegian–Greenland Sea basins. The *Azolla* phenomenon is an unexpected and unpredictable consequence of warm climate conditions.

Acknowledgments

We thank L. Bik and N. Welters for their great support. We would like to thank J. van Tongeren in Utrecht and B.J. van Heuven in Leiden for technical support with the SEM work; and T. Brain in Kings College London for his extensive support with both TEM and SEM work during this study. We thank Nora Radionova for discussion of the palaeogeography of Western Siberia. JB thanks Arthur R. Sweet for many fruitful discussions. The samples and accompanying data for *Azolla arctica* (Collinson et al., 2009), were provided by the Integrated Ocean Drilling Program (IODP). We thank Statoil and the Canadian Geological Survey for providing samples for this study. We thank the Darwin Centre, LPP Foundation and Statoil for their financial support.

Plate 1. Illustrates the distinctive characteristics of the microspore massulae and their glochidia in *Azolla arctica* (1–6), *A. jutlandica* (7–11), *Azolla* sp. 1 (12–17) and *Azolla* sp. 2 (18–22). *A. arctica* – no hairs on lower stalk, narrow tips, fluke tips not recurved; *A. jutlandica* – hairs present on lower stalk, wide tip and wide shaft; *Azolla* sp. 1 – hairs present on lower stalk, fluke tips recurved (see arrows); *Azolla* sp. 2 – no hairs on lower stalk or massula surface (see Table 2 for more information).

Plate 2. Scanning electron microscope images of megaspore apparatuses (1,4,7,10,14) and megaspore wall surfaces (other numbers) of *Azolla arctica* (1–3), *Azolla jutlandica* (4–6), *Azolla* sp. 1 (7–9), *Azolla* sp. 2 (10–13) and *Azolla* sp. 3 (14–16) showing distinctive characteristics. *A. arctica* – wavy and undulating exoperine surface rugulate in several planes (forming a reticulum); *A. jutlandica* – exoperine surface scabrate to granulate to baculate or clavate, exoperine masses fusing in a single plane (no reticulum); *Azolla* sp. 1 – exoperine surface with rounded rugulae (2 µm in narrowest dimension), which often act as muri for a very fine-scaled reticulum; *Azolla* sp. 2 – rounded rugulae (typically 1 µm), which only occasionally act as the muri for a very fine-scaled reticulum; *Azolla* sp. 3 – nine floats in two tiers, lowermost tier always visible, megaspore wall with large excrescences, exoperine surface with rounded rugulae and small papillae (less than 1 µm). (see on page 10)

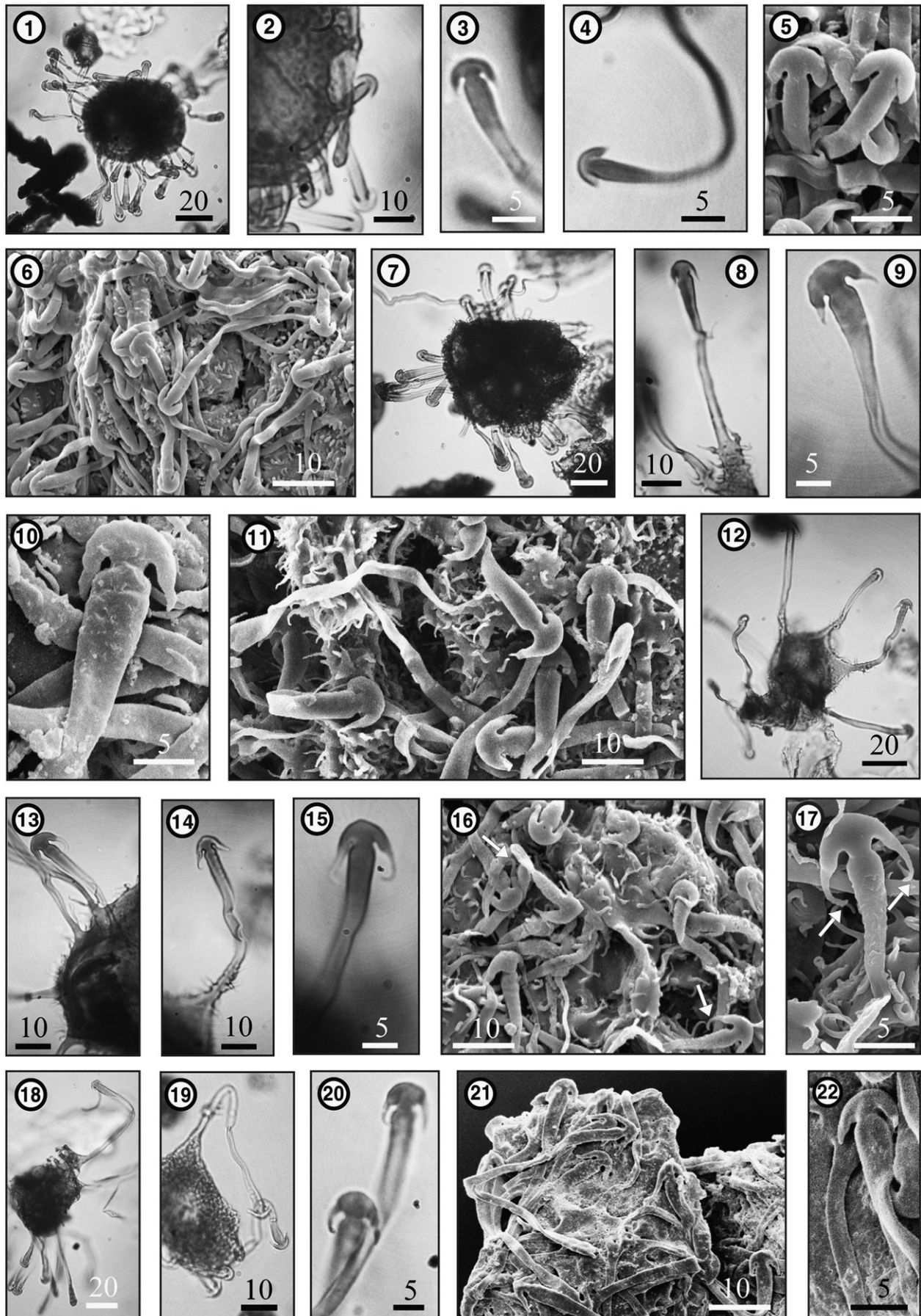


Plate 1

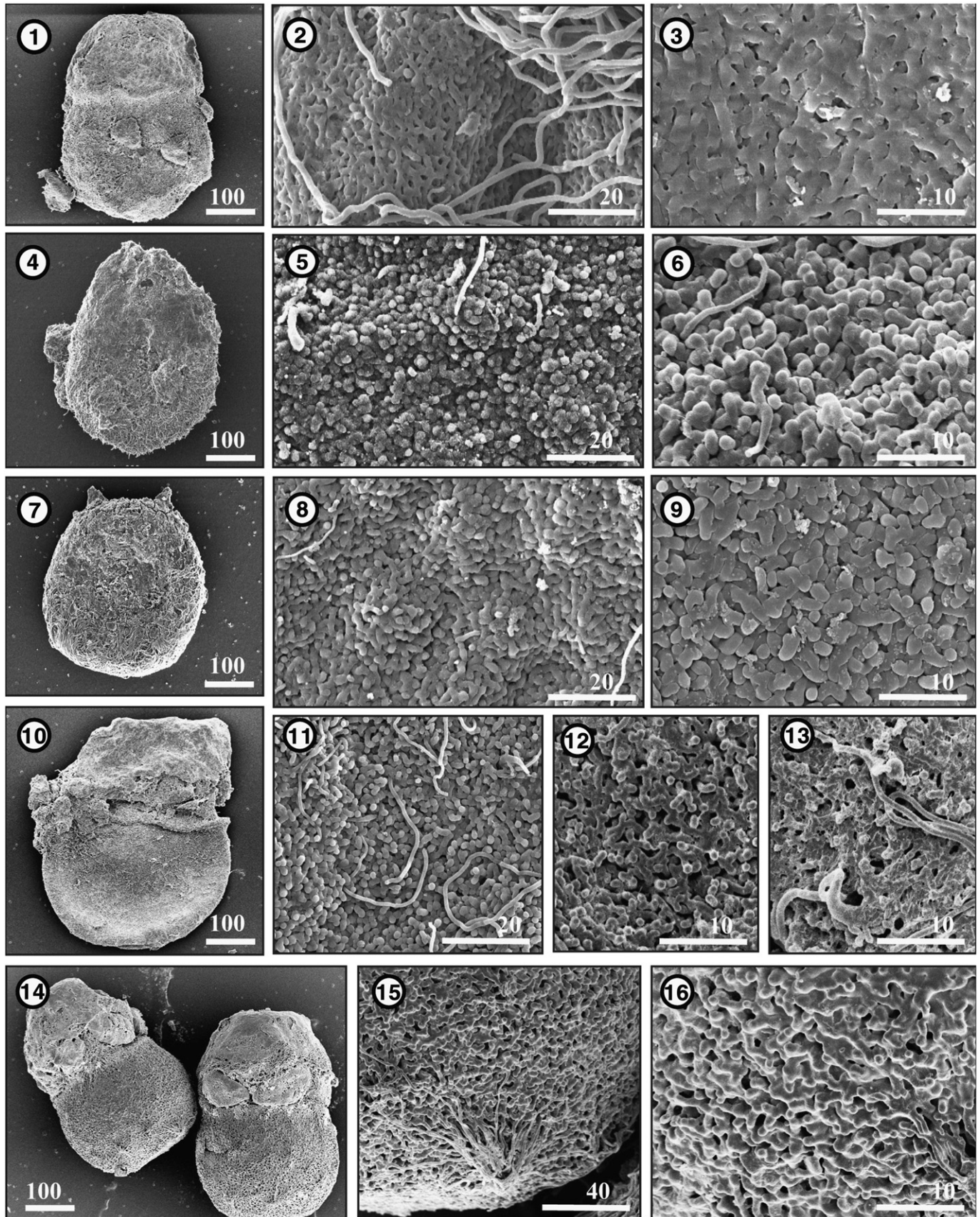


Plate 2. (caption on page 8).

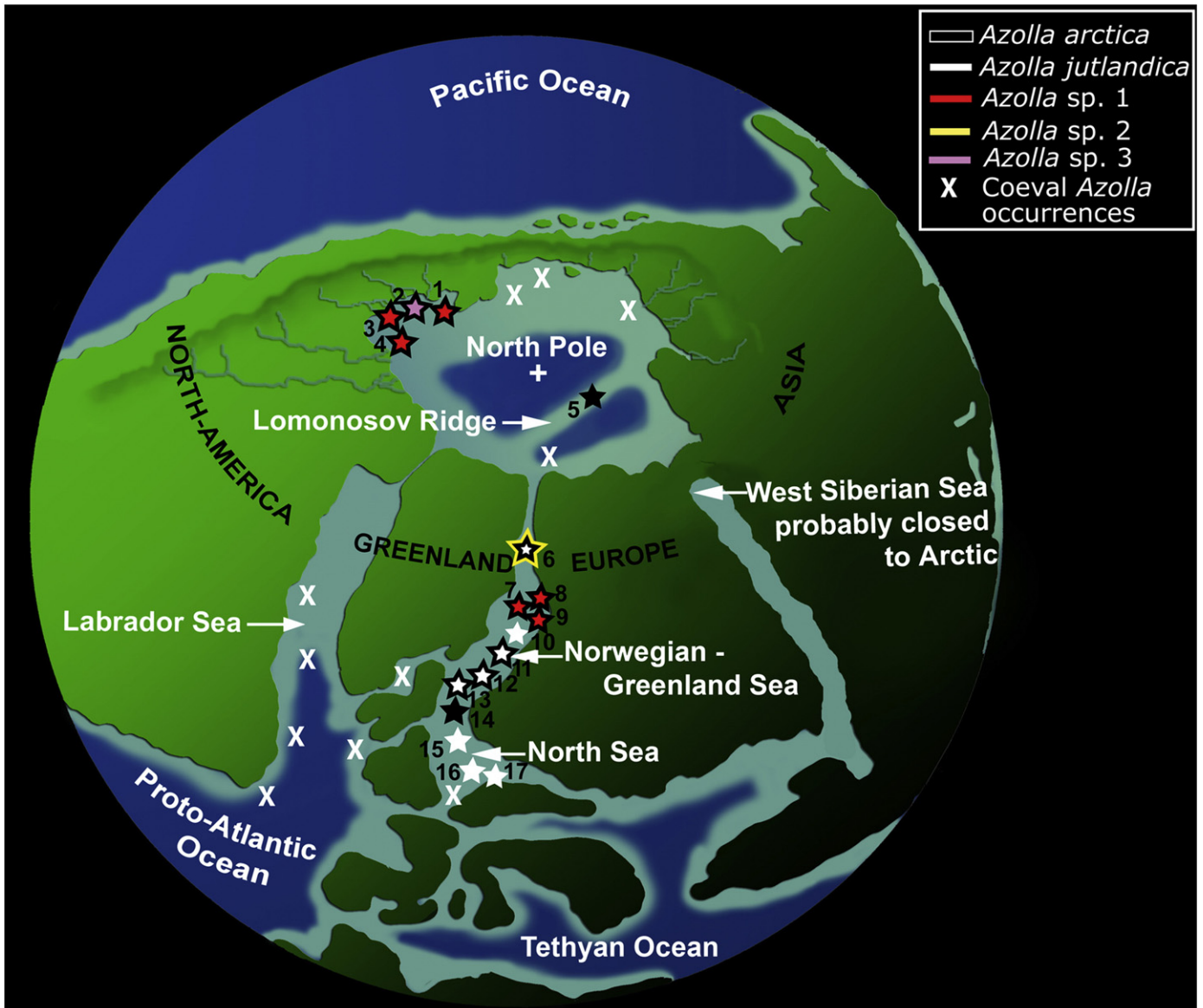


Fig. 4. Schematic palaeogeographic reconstruction (early middle Eocene; ~49 Ma; modified from Brinkhuis et al., 2006) showing the geographical distribution of the five *Azolla* species in the Arctic Ocean and Nordic Seas based on their microspore massulae and megaspore occurrences. The map is used to show the locations of seaways and land masses, but is not intended to represent their accurate palaeogeography. The West Siberian Seaway was probably briefly closed to the Arctic at least at times during the *Azolla* interval based on microfossil evidence (Radionova personal communication, Iakovleva (2011)). Coeval *Azolla* occurrences (as indicated by white crosses) relate to additional basal middle Eocene *Azolla* occurrences reported in Brinkhuis et al. (2006) and Speelman et al. (2009) and in Vandenberghe et al. (2004; *Azolla* occurrence in the Aalterbrugge Complex, Campine Basin, Belgium).

References

- Akhmetiev, M.A., Beniamovski, V.N., 2009. Paleogene floral assemblages around epicontinental seas and straits in Northern Central Eurasia: proxies for climatic and paleogeographic evolution. *Geologica Acta* 7, 297–309.
- Andreasson, F.P., Schmitz, B., Spiegler, D., 1996. Stable isotope composition ($\delta^{18}\text{O}_{\text{CO}_2}$, $\delta^{13}\text{C}$) of early Eocene fish-apatite from Hole 913B: an indicator of the early Norwegian–Greenland Sea paleosalinity. In: Thiede, J., Myhre, A.M., Firth, J.V., Johnson, G.L., Ruddiman, W.F. (Eds.), *Proc. ODP Sci. Results*, 151, pp. 583–591.
- Backman, J., Moran, K., McInroy, D.B., Mayer, L.A., the Expedition 302 Scientists, 2006. Arctic Coring Expedition (ACEX). *Proc. IODP*, 302. Integrated Ocean Drilling Program Management International, Inc., Edinburgh.
- Backman, J., Jakobsson, M., Frank, M., Sangiorgi, F., Brinkhuis, H., Stickley, C., O'Regan, M., Løvlie, R., Pålke, H., Spofforth, D., Gattacecca, J., Moran, K., King, J., Heil, C., 2008. Age model and core-seismic integration for the Cenozoic Arctic Coring Expedition sediments from the Lomonosov Ridge. *Paleoceanography* 23, PA1S03.
- Barke, J., Abels, H.A., Sangiorgi, F., Greenwood, D.R., Sweet, A.R., Donders, T., Reichart, G.-J., Lotter, A.F., Brinkhuis, H., 2011. Orbitally-forced *Azolla* blooms and middle Eocene Arctic hydrology: clues from palynology. *Geology* 39, 427–430.
- Brinkhuis, H., Schouten, S., Collinson, M.E., Sluijs, A., Sinninghe Damste, J.S., Dickens, G.R., Huber, M., Cronin, T.M., Onodera, J., Takahashi, K., Bujak, J., Stein, R., van der Burgh, J., Eldrett, J.S., Harding, I.C., Lotter, A.F., Sangiorgi, F., van Konijnenburg-van Cittert, J.H.A., de Leeuw, J.W., Matthiessen, J., Backman, J., Moran, K., the Expedition 302 Scientists, 2006. Episodic fresh surface waters in the Eocene Arctic Ocean. *Nature* 441, 606–609.
- Bujak, J.P., Mudge, D., 1994. A high resolution North Sea Eocene dinocyst zonation. *Journal of the Geological Society of London* 151, 449–462.
- Collinson, M.E., 2001. Cainozoic Ferns and their distribution. *Brittonia* 53, 173–235.
- Collinson, M.E., 2002. The ecology of Cainozoic ferns. *Review of Palaeobotany and Palynology* 119, 51–68.
- Collinson, M.E., Barke, J., van der Burgh, J., van Konijnenburg-van Cittert, J.H.A., 2009. A new species of the freshwater fern *Azolla* (Azollaceae) from the Eocene Arctic Ocean. *Review of Palaeobotany and Palynology* 155, 1–14.
- Collinson, M.E., Barke, J., van der Burgh, J., van Konijnenburg-van Cittert, J.H.A., Heilmann-Clausen, C., Howard, L.E., Brinkhuis, H., 2010. Did a single species of Eocene *Azolla* spread from the Arctic Basin to the southern North Sea? *Review of Palaeobotany and Palynology* 159, 152–165.
- Eldholm, O., Myhre, A.M., Thiede, J., 1994. Cenozoic tectono-magnetic events in the North Atlantic: Potential palaeoenvironmental implications. In: Boulter, M.C., Fisher, H.C. (Eds.), *Cenozoic plants and climates of the Arctic*. NATO ASI Series I, 27. Springer-Verlag, Berlin, pp. 35–55.
- Eldrett, J.S., Harding, I.C., Firth, J.V., Roberts, A.P., 2004. Magnetostratigraphic calibration of Eocene–Oligocene dinoflagellate cyst biostratigraphy from the Norwegian–Greenland Sea. *Marine Geology* 204, 91–127.

- Fensome, R.A., Williams, G.L., 2004. The Lentin and Williams Index of fossil dinoflagellates. American Association of Stratigraphic Palynologists Contribution Series 42, 909.
- Gradstein, F.M., Luterbacher, H.P., Ali, J.R., Brinkhuis, H., Gradstein, F.M., Hooker, J.J., Monechi, S., Ogg, J.G., Powell, J., Röhl, U., Sanfilippo, A., Schmitz, B., 2004. The paleogene period. In: Gradstein, F.M., Ogg, J.G., Smith, A.G. (Eds.), *A Geologic Time Scale*. Cambridge University Press, Cambridge, UK, p. 396.
- Greenwood, D.R., Basinger, J.F., Smith, R.Y., 2010. How wet was the Arctic Eocene rain-forest? Estimates of precipitation from Paleogene Arctic macrofloras. *Geology* 38, 15–18.
- Heilmann-Clausen, C., 1988. The Danish Subbasin, Paleogene dinoflagellates. *Geologisches Jahrbuch A* 100, 339–343.
- Heilmann-Clausen, C., 1993. Gradual morphological changes in some dinoflagellate cysts from the Eocene (Lower Tertiary) of the North Sea Basin. *Palynology* 17, 91–100.
- Heilmann-Clausen, C., Nielsen, O.B., Gersner, F., 1985. Lithostratigraphy and depositional environments in the Upper Paleocene and Eocene of Denmark. *Bulletin of the Geological Society of Denmark* 33, 287–323.
- Held, I.M., Soden, B.J., 2006. Robust Responses of the Hydrological Cycle to Global Warming. *Journal of Climate* 19, 5686–5699.
- Huber, M., Sloan, L.C., Shellito, C.J., 2003. Early Paleogene oceans and climate: a fully coupled modeling approach using the NCAR CCSM. In: Wing, S.L., Gingerich, P.D., Schmitz, B., Thomas, E. (Eds.), *Causes and Consequences of Globally Warm Climates in the Early Palaeogene*, 369. GSASP, Boulder, Colorado, pp. 25–47.
- Iakovleva, I.A., 2011. Palynological reconstruction of the Eocene marine palaeoenvironments in south of Western Siberia. *Acta Palaeobotanica* 51, 229–248.
- Jakobsson, M., Backman, J., Rudels, B., Nycander, J., Frank, M., Mayer, L., Jokat, W., Sangiorgi, F., O'Regan, M., Brinkhuis, H., King, J., Moran, K., 2007. The early Miocene onset of a ventilated circulation regime in the Arctic Ocean. *Nature* 447, 986–990.
- Miller, K.G., Wright, J.D., Browning, J.V., 2005. Visions of ice sheets in a greenhouse world. *Marine Geology* 217, 215–231.
- Moore, P.D., Webb, J.A., Collinson, M.E., 1991. *Pollen Analysis*, second ed. Blackwell Scientific Publications, Oxford, UK.
- Onodera, J., Takahashi, K., Jordan, R.W., 2008. Eocene silicoflagellate and ebridian paleoceanography in the central Arctic Ocean. *Paleoceanography* 23, PA1S15.
- Pagani, M., Pedentchouk, N., Huber, M., Sluijs, A., Schouten, S., Brinkhuis, H., Sinnighe Damsté, J.S., Dickens, G.R., the IODP Expedition 302 Scientists, 2006. Arctic hydrology during global warming at the Palaeocene-Eocene thermal maximum. *Nature* 442, 671–675.
- Pearson, P.N., Palmer, M.R., 2000. Atmospheric carbon dioxide concentrations over the past 60 million years. *Nature* 406, 695–699.
- Pross, J., Brinkhuis, H., 2005. Organic-walled dinoflagellate cysts as paleoenvironmental indicators in the Paleogene; a synopsis of concepts. *Paläontologische Zeitschrift* 79, 53–59.
- Radionova, E.P., Khokhlova, I.E., 2000. Was the North Atlantic connected with the Tethys via the Arctic in the early Eocene? Evidence from siliceous plankton. *GFF* 122, 133–134.
- Roberts, C.D., LeGrande, A.N., Tripathi, A.K., 2009. Climate sensitivity to Arctic seaway restriction during the early Paleogene. *EPSL* 286, 576–585.
- Sangiorgi, F., Brumsack, H.-J., Willard, D.A., Schouten, S., Stickley, C.E., O'Regan, M., Reichart, G.-J., Sinnighe Damsté, J.S., Henk Brinkhuis, H., 2008. A 26 million year gap in the central Arctic record at the greenhouse-icehouse transition: Looking for clues. *Paleoceanography* 23, PA1S04.
- Sluijs, A., Brinkhuis, H., 2009. A dynamic climate and ecosystem state during the Paleocene-Eocene Thermal Maximum – inferences from dinoflagellate cyst assemblages at the New Jersey Shelf. *Biogeosciences* 6, 1755–1781.
- Sluijs, A., Pross, J., Brinkhuis, H., 2005. From greenhouse to icehouse; organic-walled dinoflagellate cysts as paleoenvironmental indicators in the Paleogene. *Earth-Science Reviews* 68, 281–315.
- Sluijs, A., Röhl, U., Schouten, S., Brumsack, H.-J., Sangiorgi, F., Sinnighe Damsté, J.S., Brinkhuis, H., 2008. Arctic late Paleocene–early Eocene paleoenvironments with special emphasis on the Paleocene-Eocene thermal maximum (Lomonosov Ridge, IODP Exp. 302). *Paleoceanography* 23, 1–17.
- Speelman, E.N., Sewall, J.O., Noone, D.C. van Kempen, M.M.L., Sinnighe Damsté, J.S., Reichart, G.-J., in press. Reconstruction of Eocene Arctic hydrology using proxy data and isotope modeling. *Paleoceanography*.
- Speelman, E.N., van Kempen, M.M.L., Barke, J., Brinkhuis, H., Reichart, G.-J., Smolders, A.J.P., Roelofs, J.G.M., Sangiorgi, F., de Leeuw, J.W., Lotter, A.F., Sinnighe Damsté, J.S., 2009. The Eocene Arctic *Azolla* bloom: environmental conditions, productivity and carbon drawdown. *Geobiology* 7, 155–170.
- Speelman, E.N., Sewall, J.O., Noone, D., Huber, M., von der Heydt, A., Sinnighe Damsté, J.S., Reichart, G.-J., 2010. Modeling the influence of a reduced equator-to-pole sea surface temperature gradient on the distribution of water isotopes in the Early/Middle Eocene. *EPSL* 298, 57–65.
- Stein, R., Boucsein, B., Meyer, H., 2006. Anoxia and high primary production in the Paleogene central Arctic Ocean: First detailed records from Lomonosov Ridge. *Geophysical Research Letters* 33, L18606.
- Stickley, C.E., Koç, N., Brumsack, H.J., Jordan, R.W., Suto, I., 2008. A siliceous microfossil view of middle Eocene Arctic paleoenvironments: A window of biosilica production and preservation. *Paleoceanography* 23, PA1S14.
- Thiede, J., Myhre, A.M., Firth, J.V., Johnson, G.L., Ruddiman, W.F., 1996. Introduction to the North Atlantic-Arctic gateways: plate tectonic-paleoceanographic history and significance. *Proceedings ODP Science Results* 151, 3–23.
- Vandenbergh, N., van Simaey, S., Steurbaut, E., Jagt, J.W.M., Felder, P.J., 2004. Stratigraphic architecture of the Upper Cretaceous and Cenozoic along the southern border of the North Sea Basin in Belgium. *Netherlands Journal of Geosciences* 83, 155–171 (= *Geologie en Mijnbouw*).
- Waddell, L.M., Moore, T.C., 2008. Salinity of the Eocene Arctic Ocean from oxygen isotope analysis of fish bone carbonate. *Paleoceanography* 23, PA1S12.
- Westerhold, T., Röhl, U., 2009. High resolution cyclostratigraphy of the early Eocene – new insights into the origin of the Cenozoic cooling trend. *Climate of the Past* 5, 309–327.
- Wood, G.D., Gabriel, A.M., Lawson, J.C., 1996. Palynological techniques – processing and 906 microscopy. In: Jansonius, J., McGregor, D.C. (Eds.), *Palynology: Principles and 907 Applications*, 1. American Association of Stratigraphic Palynologists Foundation, 908 Dallas, TX, pp. 29–50.
- Zachos, J., Pagani, M., Sloan, L., Thomas, E., Billups, K., 2001. Trends, Rhythms, and Aberrations in Global Climate 65 Ma to Present. *Science* 292, 686–693.
- Zachos, J.C., Dickens, G.R., Zeebe, R.E., 2008. An early Cenozoic perspective on greenhouse warming and carbon-cycle dynamics. *Nature* 451, 279–283.